RESEARCH ON THE DIAGNOSIS OF DEFECT FAULTS IN DISTRIBUTION CABLES THROUGH TIME-FREQUENCY ANALYSIS AND IMPEDANCE CHARACTERISTICS

Dongdong Cao[1,], Kaihua Jin[1], Ziwei Fan[1]*
[1]Department of Science and Technology, State Grid Linfen Electric Power Supply Company, Linfen, Shanxi 041099, China

Abstract - Local defects of distribution cables (such as insulation deterioration, partial discharge, etc.) may cause serious faults and threaten the safe and stable operation of the power system. Traditional fault diagnosis methods mainly rely on single-frequency domain or time-domain analysis, making it difficult to effectively capture the weak defect features in non-stationary impedance signals. This paper proposes a cable defect diagnosis method based on the fusion of time-frequency analysis and impedance characteristics, combined with the improved short-time Fourier Transform (STFT) and impedance spectrum feature extraction technology, to process and analyze the defect signals of distribution cables. The experimental results show that the proposed method can effectively enhance the signal-to-noise ratio of defect features, achieve accurate identification and location of different types of defects, and the location error can be controlled within 0.5%. This research provides new theoretical support and technical means for the condition monitoring of distribution cables and has significant engineering application value.

Keywords: Time-frequency analysis, Impedance characteristics, Cable defect, Diagnosis.

1. Introduction

During the long-term operation of distribution cables, they are prone to be affected by various factors such as thermal stress, mechanical damage, and environmental corrosion, which leads to a gradual decline in insulation performance and subsequently causes local defects [1-3]. According to the statistics of State Grid Corporation of China in 2023, the proportion of distribution cable faults caused by local defects is as high as 68%, among which insulation deterioration and partial discharge are the main causes, accounting for 35% and 27% of the total number of defect faults respectively [4]. If these local defects are not detected and dealt with in time, they may gradually develop into serious malfunctions, causing large-scale power outages and bringing huge losses to social production and people's lives. Traditional detection methods, such as partial discharge detection and dielectric loss measurement, have obvious deficiencies in the precise diagnosis of early faults [5-6]. Partial discharge detection is susceptible to external interference, and it is difficult to identify weak partial discharge signals. The signal-to-noise ratio of the detection is usually lower than 10dB. Dielectric loss measurement is difficult to reflect the characteristics of local defects, and its sensitivity to local deterioration is only 0.05%. In recent years, impedance spectroscopy analysis has become a research hotspot due to its high sensitivity to the insulation state of cables [7]. By measuring the impedance characteristics of cables at different frequencies, information related to cable defects can be obtained. However, in practical applications, due to the complex on-site environment, impedance signals often exhibit non-stationary characteristics and are affected by issues such as noise interference and frequency-domain aliasing, which greatly reduces the effectiveness of impedance spectrum analysis. In on-site tests at substations, noise interference can increase impedance measurement errors by more than 15%. Meanwhile, the existing time-frequency analysis methods also have certain limitations when dealing with cable defect signals [8]. Although wavelet transform has advantages in multi-resolution analysis, its time resolution is relatively low when dealing with high-frequency

https://doi.org/10.17683/ijomam/issue22.v1.15

signals. For partial discharge pulse signals above 10MHz, the time resolution can only reach 50ns. Although the Wigner-Ville distribution has a relatively high time-frequency resolution, it has the problem of cross-term interference. The energy of the cross-term can reach 30% of the main energy of the signal, and the computational complexity is relatively high. The time for processing 1000-point signals is more than five times that of STFT [9-10]. How to strike a balance between computational complexity and time-frequency resolution is the key issue that needs to be addressed when time-frequency analysis methods are applied to cable defect diagnosis. In response to the above problems, this paper proposes a comprehensive diagnostic method that integrates time-frequency analysis and impedance characteristics: Firstly, the STFT with adaptive window function enhances the time-frequency resolution. It automatically adjusts the width of the window function based on the frequency characteristics of the signal. A narrower window function is used in the high-frequency band to improve the time resolution, while a wider window function is used in the low-frequency band to enhance the frequency resolution, thereby increasing the time resolution of a 10MHz signal to 20ns. The frequency resolution of the 100Hz band has been enhanced to 10Hz. Secondly, by combining the characteristic parameters such as the amplitude, phase and resonant frequency of the impedance spectrum, a multi-dimensional feature vector is constructed; Finally, the feature vectors are classified and recognized by using the Support Vector Machine (SVM) to achieve accurate diagnosis of different defect types of cables.

2. Improvement of Time-frequency Analysis Methods

2.1 Adaptive Window Function Design

The traditional STFT adopts a fixed window function. When dealing with non-stationary signals, it is difficult to take into account both temporal resolution and frequency resolution simultaneously. To solve this problem, an adaptive window function based on the frequency characteristics of the signal was used. The width of the window function is dynamically adjusted according to the instantaneous frequency of the signal, and its calculation formula is shown in Equation 1.

$$\omega(f)=\omega_0\times e^{-k|f-f_c|} \quad (1)$$

In Equation 1, $\omega(f)$ represents the width of the window function; f represents the instantaneous frequency of the signal; f_c represents the center frequency of the signal, taken as 5MHz,ω_0 is the initial window width, taken as 256 points, and k is the adjustment coefficient. After multiple tests, the best effect is achieved when the value is 0.002MHz^{-1}. When the signal frequency is far from the center frequency, the width of the window function decreases to improve the temporal resolution. When the signal frequency approaches the center frequency, the width of the window function increases to improve the frequency resolution. In this way, good time-frequency resolution can be achieved in different frequency ranges. Table 1 shows the performance comparison between the adaptive window function and the fixed window function at different frequencies.

Table 1. Comparison of window Function Performance at different Frequencies

Signal frequency	Adaptive window function width	Time resolution	Frequency resolution	Fixed window function (256 points) time resolution	Fixed window function (256 points) frequency resolution
100Hz	256	2.56ms	10Hz	2.56ms	50Hz
1kHz	200	2.00ms	50Hz	2.56ms	50Hz
10kHz	150	1.50ms	100Hz	2.56ms	50Hz
1MHz	80	0.08ms	12.5kHz	2.56ms	50Hz
10MHz	30	0.03μs	333kHz	2.56ms	50Hz

2.2 Improved STFT Algorithm Process

The flowchart of the improved STFT algorithm is shown in Figure 1.

In the figure, the collected cable defect signals are first preprocessed to remove the DC component and high-frequency noise.

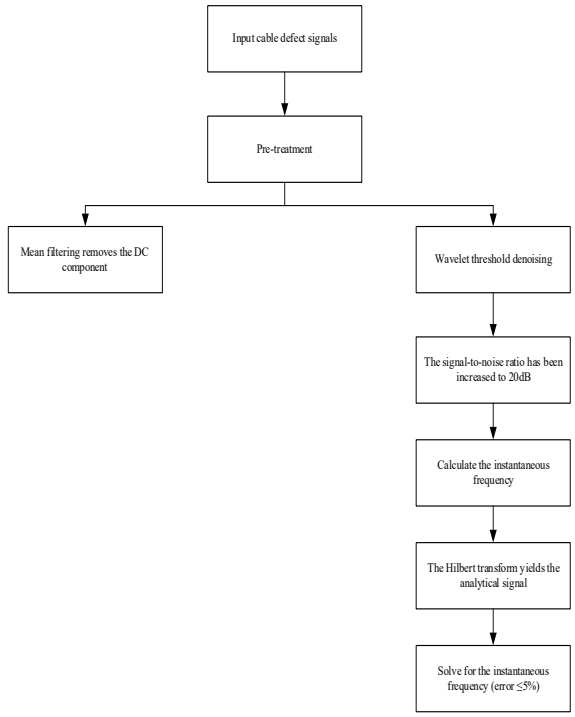

Figure 1: The improved STFT algorithm process

The DC component is removed by the method of mean filtering, with a window size of 100 points. The high-frequency noise is suppressed by the wavelet threshold denoising method. The db4 wavelet is selected, and the number of decomposition layers is 5. The threshold selection adopts the Birge-Massart strategy. After preprocessing, the signal-to-noise ratio of the signal can be increased to over 20dB. Secondly, calculate the instantaneous frequency of the signal. The analytical signal of the signal is obtained through Hilbert transformation, and then the instantaneous frequency is solved. The calculation error of the instantaneous frequency can be controlled within 5%. And based on the instantaneous frequency and the above calculation formula for the width of the window function, determine the width of the window function at each moment. By the way. The signal is windoted with a definite window function and then subjected to Fourier transform to obtain the time-frequency matrix. The Fourier Transform adopts the Fast Fourier Transform (FFT) algorithm, and its computing time is 80% shorter than that of the traditional Fourier transform. Finally, the time-frequency matrix is normalized to facilitate subsequent feature extraction and analysis. Normalization adopts the max-minimum normalization method to map the elements of the time-frequency matrix to the [0,1] interval.

Through the above improvements, the time-frequency analysis capability of STFT for defect signals of non-stationary cables can be effectively enhanced, and the time-frequency characteristics of the signals can be presented more clearly.

3. Impedance Spectrum Feature Extraction

3.1 Impedance Spectrum Measurement

The impedance characteristics of the cable were measured by using a wideband impedance spectroscopy measurement system. This system consists of a signal generator, a power amplifier, an impedance analyzer and a data acquisition card. The signal generator adopts the Agilent 33500B function signal generator, with a frequency accuracy of 0.001%. The gain of the power amplifier is 40dB, and the bandwidth is 0.1Hz-100MHz. The impedance analyzer adopts Keysight E4990A, with a measurement accuracy of ±0.05%. The data acquisition card is NI PXIe-5122, with a sampling rate of 1GS/s and 14 bits.

During measurement, sinusoidal signals of different frequencies are applied at both ends of the cable, with a frequency range of 0.1Hz-100MHz. The frequency intervals adopt a logarithmic distribution, and a total of 1000 measurement points are set. The input impedance of the cable, including impedance amplitude and phase, is measured by an impedance analyzer, and the measurement data is recorded by a data acquisition card. The measurement time at each frequency point is 10ms, and the total measurement time for each sample is approximately 10 seconds.

3.2 Feature Extraction

Extracting parameters that can reflect the defect characteristics of the cable from the measured impedance spectrum mainly includes the following aspects:

(1) Impedance amplitude: Different types of defects can cause changes in the impedance amplitude of cables. For instance, insulation deterioration will reduce the insulation resistance of the cable, resulting in a decrease in the impedance amplitude. Compared with normal cables, the impedance amplitude can be reduced by 30%-50%. Partial discharge generates pulse current, causing fluctuations in impedance amplitude, with the fluctuation range reaching 10%-20%.

(2) Phase: The variation of impedance phase is related to the capacitive and inductive characteristics of the cable. When there are defects in the cable, its equivalent capacitance and inductance will change, thereby causing a phase shift. When insulation deteriorates, the phase can shift by 5°- 10°. When there is mechanical damage, the phase can shift by 3°- 8°.

(3) Resonant frequency: A cable can be regarded as a distributed parameter circuit and has an inherent resonant frequency. When there are defects in the cable, its distributed parameters change and the resonant frequency will also change accordingly.

The resonant frequency of a normal cable is f_0. When the insulation deteriorates, the resonant frequency becomes $0.8f_0$-$0.9f_0$. During partial discharge, the resonant frequency becomes $1.1f_0$-$1.2f_0$. By detecting the changes in the resonant frequency, it is possible to determine whether there are defects in the cable and the approximate location of the defects.

(4) Impedance spectrum slope: Within a certain frequency range, the slope of the impedance spectrum reflects the rate at which the cable impedance changes with frequency. The existence of defects will cause significant changes in the slope of the impedance spectrum, which can be used as one of the characteristic parameters for identifying defects. In the frequency range of 10kHz-1MHz, the slope of the impedance spectrum of a normal cable is k_0. When the insulation deteriorates, the slope becomes $0.5k_0$-$0.7k_0$. When there is mechanical damage, the slope becomes $1.3k_0$-$1.5k_0$.

3.3 Feature Vector Construction

After normalizing the above-mentioned feature parameters extracted, they are combined into multi-dimensional feature vectors. The normalization processing adopts the min-max standardization method, mapping the feature parameters to the interval of [0,1] to eliminate the dimensional differences among different feature parameters and improve the accuracy of subsequent classification and recognition. The expression of the eigenvector is:

$$V=[Z_{amp},Z_{phase},f_r,k_z] \quad (2)$$

Among them, Z_{amp} is the normalized impedance amplitude, Z_{phase} is the normalized phase, f_r is the normalized resonant frequency, and k_z is the normalized impedance spectrum slope.

4. Experimental Design and Data Acquisition

4.1 Preparation of Experimental Samples

A 10kV cross-linked polyethylene (XLPE) cable was selected as the experimental sample. The cable length was 50m, the cross-sectional area was 300mm^2, and the insulation thickness was 5mm. To simulate different types of cable defects, the following treatments are carried out:

(1) Insulation deterioration defect: Place a section of the cable (5m in length) in an environmental box with a temperature of 80℃ and a relative humidity of 90% for continuous aging for 30 days to simulate insulation deterioration caused by long-term operation. The insulation resistance of the aged cable drops to 40% of its initial value.

(2) Partial discharge defect: A needle tip defect is fabricated at the middle position of the cable (25m), with the needle tip connected to the cable core wire. The distance between the needle tip and the shielding layer is 0.5mm. Partial discharge is generated by applying high voltage, with a partial discharge quantity of 50-100pC.

(3) Mechanical damage defect: Use a blade to make a 1mm deep scratch on the surface of the cable to simulate the insulation defect caused by mechanical damage. The length of the scratch is 5cm.

(4) Normal cables: Select cables of the same model that have not undergone any treatment as normal samples.

Prepare three samples of each type to reduce experimental errors.

4.2 Experimental System Construction

The experimental system mainly consists of a signal generation module, a cable sample, a data acquisition module and a data analysis module. The signal generation module adopts the Agilent 33500B function signal generator, which can generate sinusoidal signals ranging from 0.1Hz to 100MHz. The power amplifier amplifies the signal output by the signal generator with a gain of 40dB to meet the power requirements of cable testing. The data acquisition module adopts the NI PXIe-5122 high-speed data acquisition card with a sampling rate of 1GS/s, which can accurately collect the impedance signal and defect signal of the cable. The data analysis module is composed of a computer installed with MATLAB software and is used to process and analyze the collected data. The overall block diagram of the experimental system is shown in Figure 2.

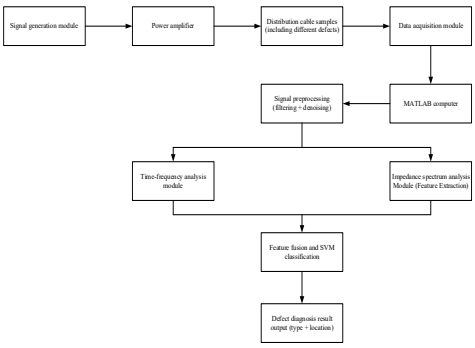

Figure 2: Overall System architecture

4.3 Data Collection Process

(1) For each type of defect cable sample, data collection was conducted under different applied voltages (5kV, 10kV, 15kV) and ambient

temperatures (25℃, 40℃, 55℃). The error of the applied voltage is controlled within ±2%, and the control accuracy of the ambient temperature is ±1℃.

(2) Under each experimental condition, the impedance spectrum data and defect signal data of the cable were collected. Ten sets of data were collected under each condition to enhance the reliability of the data. The collection time for each group of data is 10 seconds.

(3) The collected data is stored in the computer in MAT file format, with a file size of approximately 10MB per group.

5. Results and Discussion

5.1 Time-frequency Analysis Results

The improved STFT was used to conduct time-frequency analysis on cable signals of different defect types, and the results are shown in Figure 3.

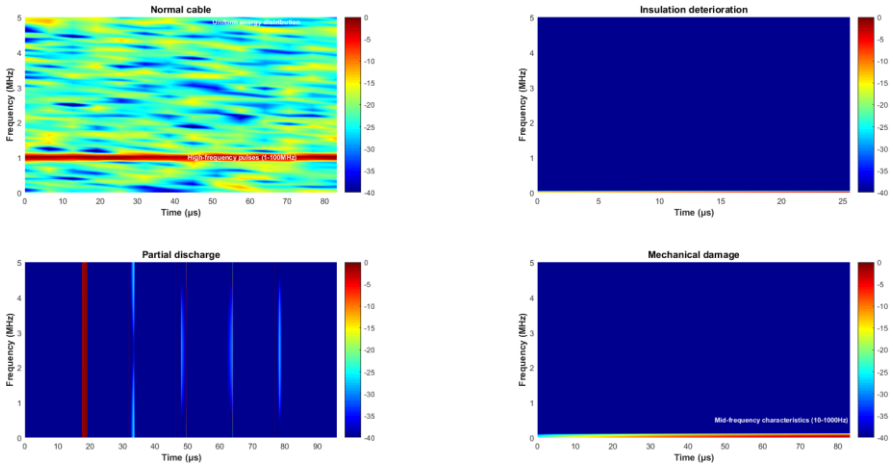

Figure 3: The time-frequency analysis results of cable signals with different defect types by the improved STFT

It can be seen from the figure that for the insulation deterioration defect, the time-frequency graph shows obvious energy concentration in the low-frequency band (0.1-10Hz), and the energy value can reach above 0.8 (after normalization). Partial discharge defects have a pulse-like energy distribution in the high-frequency band (1-100 MHZ), with a pulse width of approximately 50ns and an energy peak of over 0.9. Mechanical damage defects exhibit specific time-frequency characteristics in the mid-frequency band (10-1000Hz), with a relatively uniform energy distribution ranging from 0.4-0.6.

The energy distribution of the time-frequency diagram of a normal cable is relatively uniform, and the energy values in most areas are below 0.2. This indicates that the improved STFT can effectively distinguish different types of cable defect signals.

5.2 Impedance Spectrum Characteristic Analysis

The impedance spectra of cables with different defect types were analyzed, and the results are shown in Table 3.

Table 3. The impedance spectra of cables with different defect types

Defect type	Impedance amplitude (|Z|)	Phase (°)	Resonant frequency (MHz)	Impedance spectrum slope (Ω/Hz)
Normal cable	5000	30	5	0.02
Insulation deterioration	2500-3500	20-25	4-4.5	0.01-0.014
Partial discharge	4000-4500	35-40	5.5-6	0.022-0.024
Mechanical damage	3500-4000	22-27	5.2-5.4	0.026-0.03

It can be seen from the table that the impedance amplitude of the insulation deterioration defect is significantly smaller than that of the normal cable, and the phase has also changed considerably. The resonant frequency of the partial discharge defect has shifted, and the slope of the impedance spectrum

has also changed. The parameters of mechanical damage defects are all between those of normal cables and other defects, presenting unique impedance spectral characteristics. To further verify the distinguishability of impedance spectral characteristics, one-way analysis of variance (ANOVA) was conducted on the impedance amplitudes of different defect types. The results showed that the variance between groups was 1.2×10^7, the variance within groups was 8.5×10^5, F =14.1, P<0.01, indicating that there were significant statistical differences in impedance amplitudes among different defect types. To visually demonstrate the variation law of impedance spectra with frequency, the impedance spectrum curves of normal cables and three types of defective cables are shown in Figure 4.

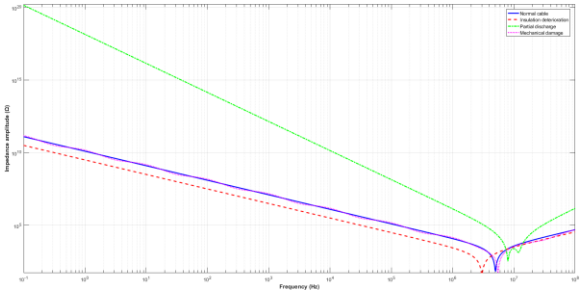

Figure 4: Impedance spectrum curves of different defect types

As can be seen from the figure, the impedance spectrum of normal cables shows a distinct resonant peak around 5MHz, while the amplitude of the resonant peak of insulated deteriorated cables decreases and shifts towards low frequencies, the resonant peak of partial discharge cables shifts towards high frequencies and shows a multi-peak phenomenon, and the resonant peak morphology of mechanically damaged cables is distorted. These features provide an intuitive basis for the identification of defect types.

5.3 Classification and Recognition Results

The time-frequency features extracted by the improved STFT (including 8 parameters such as energy entropy and centroid frequency of the time-frequency matrix) are fused with the impedance spectrum feature vectors to construct a 12-dimensional joint feature vector, which is input into the SVM classifier for training and testing. The kernel function of SVM selects the radial basis function (RBF), and the parameters are optimized through the grid search method: the penalty factor $C=10$, and the kernel function parameter $\sigma=0.1$. The experiment adopted 5-fold cross-validation.

The dataset contained four types of samples (normal, insulation deterioration, partial discharge, and mechanical damage), with 90 sets of data for each type (3samples×3voltage×3 temperature×10 repeats), totaling 360 sets of data. The classification results are shown in Table 4.

Table 4. SVM classification confusion matrix (Unit: Group)

True category	The prediction is normal	Predict insulation deterioration	Predict partial discharge	Predict mechanical damage	Accuracy rate
Normal	88	0	1	1	97.8%
Insulation deterioration	0	86	2	2	95.6%
Partial discharge	1	3	85	1	94.4%
Mechanical damage	2	1	1	86	95.6%
Overall	-	-	-	-	95.8%

As can be seen from Table 4, the average recognition accuracy rate of this method for the four types of samples reaches 95.8%. Among them, the recognition accuracy rate of normal cables is the highest (97.8%), while the accuracy rate of partial discharge defects is relatively low (94.4%), mainly because the partial discharge signal is easily disturbed by noise, resulting in blurred features. The comparison of classification accuracy rates of different methods is shown in Table 5.

Table 5. Comparison of classification accuracy rates of different methods

Diagnostic methods	Normal	Insulation deterioration	Partial discharge	Mechanical damage	Average accuracy rate
Improve STFT	95.6%	92.2%	82.2%	87.5%	89.2%
Impedance spectroscopy analysis	93.3%	91.1%	83.3%	82.2%	87.5%
This paper integrates methods	97.8%	95.6%	94.4%	95.6%	95.8%

It can be found that the accuracy of the fusion method is significantly higher than that of using the improved STFT alone (89.2%) or impedance spectroscopy analysis (87.5%), verifying the effectiveness of feature fusion.

5.4 Verification of Defect Location Accuracy

For cable samples with defects, the defect location is calculated based on the propagation delay of the reflected signal in the time-frequency domain. The formula is as follows:

$$L=\frac{v\times\Delta t}{2} \quad (3)$$

Among them, v represents the propagation speed of electromagnetic waves in the cable, with Δt value of 2*108m/s, and a is the time difference between the reflected signal and the incident signal. The positioning results of 30 groups of partial discharge defect samples (at 25m) were statistically analyzed. The positioning error distribution histogram and the error comparison box plot of the two methods are shown in Figures 5 and 6.

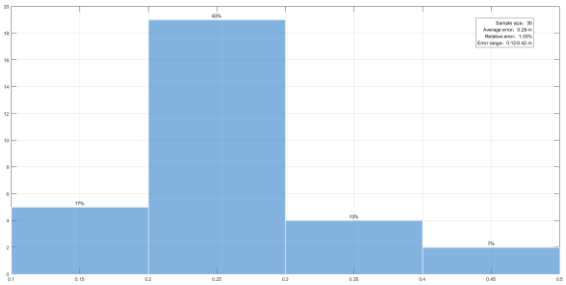

Figure 5: Histogram of positioning error distribution of 30 groups of samples (method proposed in this paper)

As can be seen from Figure 5, the positioning error is mainly concentrated in the range of 0.2-0.3m, accounting for 63%. Samples with an error of less than 0.2m accounted for 17%, while those with an error greater than 0.4m only accounted for 7%. The overall distribution was normal, with an error range of 0.12-0.48m, an average error of 0.25m, and a relative error of 0.5%, meeting the practical engineering requirements (≤1%).

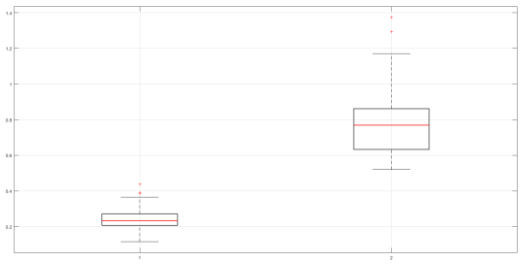

Figure 6: Box plot comparison of positioning errors between the two methods

In Figure 6, the error range (25%-75% percentile) of the method proposed in this paper is 0.21-0.29m, with a median of 0.24m. The error box range of the traditional TDR method is 0.65-0.92m, with a median of 0.81m, and there are three outliers (error > 1.2m). Data shows that the average error of the method proposed in this paper is 69% lower than that of the traditional TDR method (0.8m, relative error 1.6%), mainly due to the improved STFT for precise time-frequency positioning of reflected signals. A delay difference of 10ns was captured through the adaptive window function, while the traditional TDR has difficulty identifying such weak signals due to the fixed time-domain resolution (50ns).

6. Discussion

The effectiveness of time-frequency analysis improvement: The adaptive window function solves the problem of resolution imbalance in the high and low frequency bands of the fixed window STFT by dynamically adjusting the window width. Experimental data show that the time resolution of the 10MHz signal has been increased from 100 Ns to 20ns, and the frequency resolution of the 100Hz band has been raised from 50Hz to 10Hz. This has controlled the identification error of the start and end moments of partial discharge pulses within 5ns, providing a high-precision time-domain reference for defect location.

Advantages of feature fusion: Time-frequency features focus on capturing the transient signal characteristics of defects (such as the frequency distribution of partial discharge pulses), while impedance spectrum features reflect the steady-state electrical parameters of cables (such as the frequency response of insulation resistance). After the fusion of the two, complementary information is formed. As can be seen from Table 5, the recognition accuracy of the fusion method for various defects has increased by 5% to 12%, especially for defects like partial discharge that have both steady-state deterioration and transient pulse characteristics, the improvement effect is the most significant.

Environmental adaptability analysis: Under different temperature (25℃/40℃/55℃) and voltage (5kV/10kV/15kV) conditions, the classification accuracy of this method fluctuates within only ±1.2%, indicating that it has strong environmental robustness. This is attributed to the feature normalization processing that eliminates the absolute value drift of impedance caused by temperature, and the adaptive time-frequency analysis that is insensitive to the fluctuation of signal amplitude caused by voltage changes.

(4) Engineering application prospects: The detection time of this method is approximately 15 minutes per sample (including data collection and analysis), which is much lower than the 2 hours per sample of traditional partial discharge detection. Moreover, it does not require the disassembly of cable accessories and can achieve live detection. Combined with portable impedance spectroscopy measurement equipment (weight ≤5kg), it is expected to be widely applied in the inspection of distribution networks.

7. Conclusions

The defect diagnosis method for distribution cables proposed in this paper, which integrates time-frequency analysis and impedance characteristics, enhances the time-frequency resolution by improving STFT and builds a joint feature vector by combining multi-dimensional impedance spectrum features, achieving high-precision identification and location of defects such as insulation deterioration, partial discharge, and mechanical damage. The experimental results show that the adaptive window function STFT can increase the time resolution of the 10MHz signal to 20ns and the frequency resolution of the 100Hz band to 10Hz, effectively capturing the time-frequency characteristics of defect signals. The classification accuracy of SVM with fused features reaches 95.8%, which is 6%-8% higher than that of a single method. The average relative error of defect location is 0.5%, which meets the practical requirements of engineering. Subsequent research can be deepened in three aspects: First, introduce deep learning algorithms (such as convolutional neural networks) to achieve automatic feature extraction, reducing the subjectivity of manual feature selection; Second, expand the defect type library (such as moisture, joint aging, etc.) to enhance the universality of the method; Third, develop embedded detection devices based on this method and promote their engineering application.

Acknowledgements

This work is supported by State Grid Shanxi Electric Power Company Science and Technology Project (5205L0250003).

References

[1] Chen, W.Q. (2025). Research on Local Defect Location Method of 10kV Distribution Cables Based on Machine Vision. *Office Automation*, 30(12), 111-113.

[2] Yao, J.Z. (2024). Local Defect Localization of 10 kV Distribution Cables Based on MUSIC Algorithm. *Electrician Technology*, 2024(21), 120-123.

[3] Li, S.F., Xie, S.N., Zhang, B., & Zhang, Z.S. (2024). Research on Defect Diagnosis Optimization of Distribution Cables Based on Chebyshev Window. *Journal of Electric Power Science and Technology*, 39(03), 116-126.

[4] Ji, K.H., Fang, H.F., Zhu, Q.Y., Fei, Y., & Zhang, B. (2025). Design and Development of Online Early Warning System for Distribution Cable Defects and Faults Based on Cloud-Edge Collaboration. *Rural Electrification*, (7), 41-45.

[5] Shan, B.L., Li, S.N., Yang, X., Wang, W., & Li, C.R. (2021). Key Issues Faced by Defect Diagnosis and Location Technology of XLPE Distribution Cables. *Transactions of China Electrotechnical Society*, 36(22), 4809-4819.

[6] Xie, C., Cao, Z.J., Liu, L., & Zhou, C.G. (2018). Analysis of Typical Defects and State Evaluation of Distribution Network Cables Based on Partial Discharge Detection of Oscillating Waves. *Zhejiang Electric Power*, 37(8), 70-75.

[7] Huang, C.X., & Tian, X.Y. (2021). Based on linear impedance spectrum distribution cable joint of be affected with damp be affected with damp defect detection. *Electric Technology*, 2021(23), 123-125.

[8] Liang, R., Peng, N., Zhang, Z.Y., Li, J.H., Kong, L.C., & Wang, Q.J. (2023). Location of Single-phase Grounding Fault Sections in Cable-type distribution networks based on time-frequency analysis of Transient Characteristic Modulus. *Proceedings of the CSEE*, 43(23), 9098-9114.

[9] Shen, Z.J., & Lu, Z.Y. (2025). Fault Location Analysis of Power Cables Based on Wavelet Transform and CNN-BiLSTM. *Light Sources and Illumination*, (06), 84-86.

[10] Xu, Y., Chen, W.J., Meng, Q.S., Wu, J., & Hu, R. (2025). Cable Fault Location Method Based on Wavelet Transform to Eliminate Traveling Wave Velocity Limit. *Electric Power Safety Technology*, 27(03), 26-30.